



# Determination of tensile residual strength of fibre reinforced concrete by a robust and simple test

Luis Segura-Castillo · Renata Monte ·  
Isaac Galobardes · Antonio D. de Figueiredo

Received: 19 October 2022 / Accepted: 16 February 2024 / Published online: 25 May 2024  
© The Author(s), under exclusive licence to RILEM 2024

**Abstract** A bending test was selected by modern codes as a reference test for fibre-reinforced concrete (FRC) mechanical characterization. However, specimen dimensions, lack of laboratories adequately equipped, and its complexity hinder its use. This study aims to evaluate the so-called Montevideo (MVD) test as an alternative to the results of EN14651 bending tests, simplifying FRC mechanical evaluation. A strong correlation was obtained using the results of experimental campaigns carried out in three countries. Using two linear transformations, MVD loads can be converted to the EN14651 ones,

both for the limit of proportionality and for the residual loads, which are valid for all the CMOD reported in EN14651. These general rules seem valid for different types of concretes (conventional, Self-Compacting, Ultra High-Performance, Micro and Sprayed concrete), blended with different fibre types (plastic and steel) and a wide range of contents, which show both softening and hardening behaviour.

**Keywords** Bending test · Montevideo test · EN14651 · Synthetic fibres · Steel fibres

---

**Supplementary Information** The online version contains supplementary material available at <https://doi.org/10.1617/s11527-024-02321-1>.

---

L. Segura-Castillo (✉)  
Department of Structures, Facultad de Ingeniería,  
Instituto de Estructuras y Transporte - Oficina 105,  
University of the Republic, Julio Herrera y Reissig 565,  
11300 Montevideo, Uruguay  
e-mail: lsegura@fing.edu.uy

R. Monte · A. D. de Figueiredo  
Department of Civil Construction Engineering,  
Polytechnic School, University of São Paulo, Caixa Postal  
61548, Sao Paulo, CEP 05508-900, Brazil

I. Galobardes  
Civil Engineering Department, Xi'an Jiaotong-  
Liverpool University, 111 Ren'ai Road, Suzhou  
Industrial Park, Suzhou 215000, Jiangsu Province,  
People's Republic of China  
e-mail: igalobardes@aqu.aad

## 1 Introduction

There is a growing interest in fibre reinforced concrete (FRC) due to some improvements that the use of this type of material could provide, such as reduced construction time, labour costs and enhanced properties for structural elements, such as enhanced crack control [1]. Despite some limitations, such as the reduction of the workability of the composite with the increase of the fibre content [2], new applications regularly emerge with fibres as partial or total substitution of conventional reinforcement. The recent increase in FRC use is intensified by the introduction of fibres as a structural material by several codes, guidelines and standards in different countries (e.g. Europe [3], USA [4], Brazil [5], Australia [6], Singapore [7], *fib* [8]). In these codes, design rules are based on material characterization to obtain



constitutive equations required for the design of structural applications [9]. Regular quality control should also be established focusing on the material properties verification, to ensure the required structural performance.

The increase in the residual (post-cracking) tensile strength is the main contribution of fibres to plain concrete, which must be measured for FRC design [9]. For this, fib Model Code [8], among other recent codes, standards and recommendations (e.g. The Concrete Society TR34 [10], Spanish concrete code (EHE-08) [11], Brazil FRC standard [5], Singapore FRC standard [7], ITA report 24 [12]) have selected the three-point bending (3PB) test on a notched beam, according to EN 14651 [13], for FRC mechanical characterization. In this test, a deflection is imposed on the beam, and the load is registered for the different values of crack mouth opening displacement (CMOD), which are measured by a clip gage positioned in the notch. Alternatively, deflection can be measured instead of the CMOD. According to the EN14651 standard [13], four values of the residual strength ( $f_{R1}$ ,  $f_{R2}$ ,  $f_{R3}$ , and  $f_{R4}$ ) should be calculated and reported, corresponding to a CMOD of 0.5, 1.5, 2.5 and 3.5 mm, respectively.

The design codes provide rules to convert these residual strengths obtained in the bending test to constitutive equations, which can be used for the design of FRC elements. Only two values of residual strength are usually used (one associated with the service limit state—SLS and the other for ultimate limit state—ULS analysis). Many codes, including the fib Model Code, have selected  $f_{R1}$  and  $f_{R3}$  for the FRC classification, but there are examples of other choices, such as TR34 [10] for designing FRC in industrial pavements, which has selected  $f_{R1}$  and  $f_{R4}$  instead.

Despite the increase in the use of engineering principles for the design of FRC, there are technological restrictions as well as practical drawbacks that hinder the use of the EN14651 test, namely: (a) the specimen dimensions (150×150×550 mm) eventually make its weight high, around 30 kg, which makes its handling difficult and increases the risk of occupational injuries; (b) it is practically impossible to extract large prismatic cores from existing structures, which may be needed to investigate deficiencies detected under the service life or directly from a non-conforming quality control evaluation under its construction; (c) there is a lack of laboratories adequately equipped

with the testing machines required for the EN14651 test, i.e. with a closed loop displacement control system; (d) specific testing machine and the use of clip gage make EN14651 a complex test with a difficult execution, which requires specialised technicians.

With these drawbacks under consideration, several codes [5, 8, 11] allow the use of other tests for the quality control of FRC if a correlation can be established between the proposed test and EN14651. Alternative tests that can be conducted in simpler and faster ways to facilitate the control system were already proposed, minimizing some of the drawbacks explained before, such as the Montevideo (MVD) test [14]; the double punch or Barcelona test (BCN) [15]; or the double-edge wedge-splitting (DEWS) test [16].

All the aforementioned use compact specimens, usually smaller than 4 L, always weighing <10 kg. The use of smaller specimens has some advantages, such as material saving, simplified execution, the possibility of testing cores, and even evaluating the effect of fibre orientation. However, some tests also present drawbacks, such as post-peak instabilities in DEWS and BCN, due to unstable crack propagation, which results in a lack of information regarding small crack openings [17–20]. Also, the BCN test is based on a complex failure mechanism, and the DEWS test has a complex specimen preparation.

Several attempts were made to correlate beam test results with the other types of tests (including the BCN test [17, 21, 22], DEWS test [21], and panels tests [23–25]), with different degrees of success. One drawback found in these works is that the equations obtained to correlate the results could not be generalized for all FRC composites, requiring a personalised correlation for each mix, or a less accurate general correlation [17, 21, 23]. Also, analysis of the BCN test showed that due to the more complex nature of the test, parameters such as force and energy are needed in the correlation, which is not valid for low CMOD values, due to the aforementioned post-peak instabilities [17, 18, 22].

Many similarities were found between the MVD and the EN14651 test in preliminary tests [14]. Both tests have the same testing area (150×125 mm), and they obtain a qualitatively similar cracking pattern (vertically inverted), i.e. a crack that starts at the notch end and propagates towards the base of the specimen. Load-CMOD curves are also qualitatively similar in both tests. Also, previous results have shown a stable



crack propagation in the MVD test, even when small open-loop testing machines are used. However, more tests were needed to consolidate a robust and general correlation between their results. In that sense, the objective of this study was to evaluate the capacity of the Montevideo (MVD) test to predict the results of the 3PB test, performed by the EN14651 standard. The goal was to obtain a robust correlation between the MVD and the 3PB tests, which may be used for FRC mechanical characterization for structural applications. For this, experimental campaigns were carried out in three different countries using 22 different types of FRC mixes with varying matrices, types of fibres and test set-ups.

## 2 Montevideo test

### 2.1 Test set-up

The MVD test [14] is mainly based on the wedge-splitting test (WST) [26], but some changes are introduced to simplify it to make it a viable test for routine quality control, namely: smaller test specimens, simpler testing machines and reduced specimen preparation. In addition, this method is intended to be potentially applicable to specimens prepared from extracted cores. The complex load mechanism of the WST is substituted by only a wedge (Fig. 1a). The specimen geometry and its preparation are thus also reduced to just a notch, with the same cross-section dimensions (Fig. 1d) as the specimen of the EN14651 test [14]. This notch could be executed in cast or extracted specimens. An image during the test is shown in Fig. 1b.

Steel pieces are glued to the notch sides to provide a steel-to-steel contact (Fig. 1c). Immediately before starting the test, a multi-function lubricant (e.g. WD-40) is applied to the contact surface to reduce friction. This contact preparation minimizes any damage to the wedge and the specimen, allowing testing FRC with softening or hardening behaviour. Also, it produces a more stable friction coefficient, obtaining a stable opening force acting towards the specimen, reducing intrinsic uncertainties and scatter, besides producing smaller loads during the test.

Post-peak instability probabilities are increased when testing machines with low stiffness are used (which provide greater energy transfer to the

specimen) and when FRC with low residual strengths are tested [27]. Although closed-loop systems can counteract these deficiencies, there still have been cases reported in which instabilities occur with these systems [28].

On the other hand, in open systems, instabilities are more common, also worsening when machines with low stiffness are used and when FRC with low fibre contents are tested [20].

No instabilities or abrupt failures were registered in more than a hundred MVD tests performed so far, even in the cases that are known to provoke instabilities: FRC with low plastic fibre contents; using small testing machines, like the usually used in CBR tests (see Fig. 3d); or performing the test controlled by the stroke displacement (open system) of the testing machine. The reduced possibility of a post-peak instability may be due to the reduced loads used in the test, especially at peak load (In the BCN test peak load ranges from 150 and 300 kN [29, 30], whereas in the Montevideo test it ranges between 10 and 20 kN [14, 31]), and the smaller amount of energy stored in the specimen in a WST [32].

Two different set-ups for the test were used, as shown in Fig. 1e. First, tests were carried out with a “Fixed” wedge, restricting the movement of the wedge in contact with the plate of the test machine. Therefore, the wedge was not allowed to move during the test. In this set-up, the wedge most likely had an uneven contact with the notch borders, producing an unsymmetric bending in the specimen. To avoid this uncertainty, a steel roller was placed between the wedge and the test machine plate, allowing a free rotation of the wedge in its main plane. This set-up, called “Hinged”, allows a smoother application of the force to the specimen.

### 2.2 Crack mouth opening displacement

The MVD test can be controlled by the stroke displacement ( $\delta$ ) of the test machine. This is possible in most electromechanical testing machines, since they usually have a crosshead displacement sensor, and in servo-controlled hydraulic presses which have an internal crosshead displacement sensor. A constant speed (0.5 mm/min) was used in general for the tests. The required displacement needed to complete the test is usually around 10 mm; therefore, the running time of the test is around 20 min. In Fig. 2a, a typical

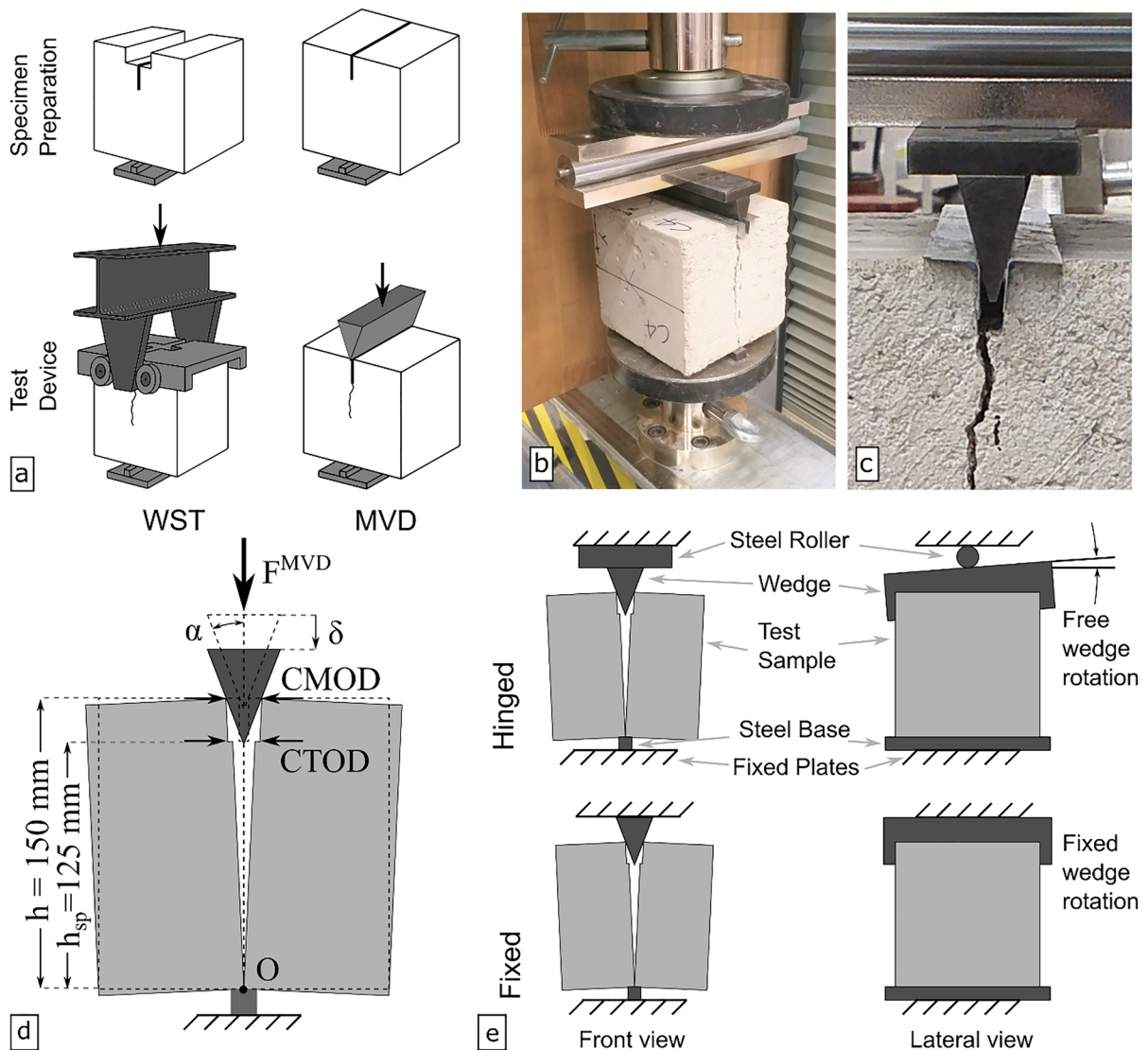


**Fig. 1** a Comparison of MVD and WST tests (adapted from [14]); b MVD test set-up; c detail of wedge and steel corners contact; d dimensions parameters and kinematic idealization; e hinged and fixed set-up of the test

Load vs. Stroke Displacement result for the MVD test is shown in the dark line. The result corresponds to a FRC with softening behaviour. Crack Mouth Opening Displacements (CMOD) vs. Stroke Displacement are also plotted in Fig. 2a in a grey line.

The two differential stages that characterize the MVD test are marked in Fig. 2. The first stage takes place from the start of the test until the initiation of cracking in the matrix ( $\delta_0$ ). In the first stage, the wedge penetration into the notch gradually increases the applied load. While relatively large

displacements of the stroke take place (with values from approximately 1 to up to 3 mm), the CMOD is negligible as only elastic strains develop, which are very small compared to the post-crack ones. Therefore, the entire first stage is discarded in the test analysis. The first stage finishes when the concrete matrix reaches the tensile strength and a crack is formed in the matrix, turning the specimen into two rigid bodies rotating over the base of the specimen (Point “O” in Fig. 1d). In the second stage, for FRC with softening behaviour (Fig. 2a), there is a

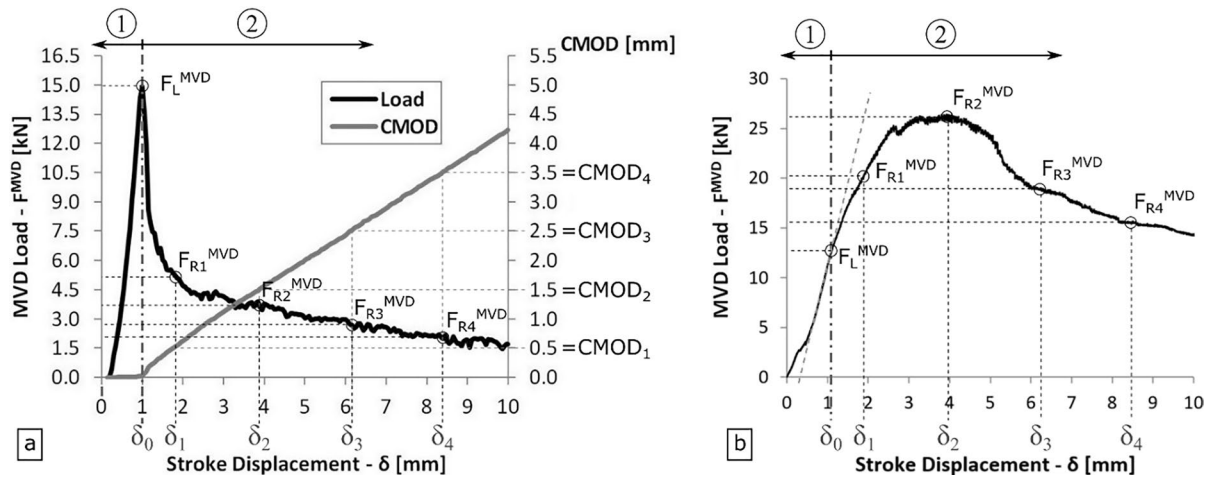


**Fig. 2** **a** Typical Load and CMOD versus displacement curve for softening FRC; **b** typical load versus displacement curve for hardening FRC

load drop as the fibres bridge the crack and take the loads.

After cracking, a linear correlation can be seen between the CMOD and the stroke displacement. The relationship follows the theoretical model obtained under the rigid body assumption, which allows the extrapolation of the results also to the Crack Tip Opening Displacement (CTOD) [14]. The displacement in which the crack is formed ( $\delta_0$ , see Fig. 2a) was also shown [14] to approximately correspond to the peak load for FRC with softening behaviour. Therefore, the CMOD values of the test can be directly calculated based on the aforementioned parameters and the wedge geometry, with the following equation:

$$CMOD = (\delta - \delta_0) \cdot 2 \cdot \tan \alpha \quad (1)$$

where  $\alpha$  is the angle between the wedge side and the vertical direction (Fig. 1d). Considering the wedge angle proposed ( $\alpha = 15^\circ$ ), Eq. 1 yields:

$$CMOD = (\delta - \delta_0) \cdot 0.536 \quad (2)$$

In particular, the four  $CMOD_i$  used in the 3PB test according to the EN14651 standard ( $CMOD = 0.5, 1.5, 2.5$  and  $3.5$  mm, corresponding to  $i = 1, 2, 3$  and  $4$ , respectively) corresponds to four stroke displacements ( $\delta_i$ ), which can be directly calculated once  $\delta_0$  is determined. The usual values of  $CMOD$  and  $\delta_i$  used in the 3PB and MVD tests are summarized

**Table 1** Usual  $CMOD_i$  and  $\delta_i$  for EN14651 and MVD tests

$i$	$CMOD_i$ [mm]	$\delta_i$ [mm]
L	0.0	$\delta_0$
1	0.5	$0.93 + \delta_0$
2	1.5	$2.80 + \delta_0$
3	2.5	$4.66 + \delta_0$
4	3.5	$6.53 + \delta_0$
*	4.0	$7.46 + \delta_0$

\*End of test

in Table 1 and represented in Fig. 2. Controlling the test by the stroke displacement allows for avoiding a direct crack opening measure (e.g. with clip gages) or an external displacement measure (e.g. by a linear transducer), reducing preparation labour and possible experimental errors.

For FRC with hardening behaviour (Fig. 2b), it is possible to use the same equations. However, as in this case, the beginning of the cracking does not correspond to the peak load, it may be difficult to evaluate the displacement at the first crack ( $\delta_0$ ). This difficulty may also be found in flexural tests performed with FRC with strain hardening behaviour. One possibility is evaluating the change in the slope of the plot. When the matrix cracks, the slope decreases, indicating the end of stage 1. Alternatively, a direct measure of CMOD may be used.

### 2.3 Residual load

$F_{Ri}^{MVD}$  Is the load corresponding with each  $CMOD = CMOD_i$  or  $\delta = \delta_i$  ( $i=1, 2, 3, 4$ ), and  $F_L^{MVD}$  is the load corresponding to the LOP or  $\delta = \delta_0$ . All of them are also represented in Fig. 2. The proposal is that MVD test loads, both for the residual loads ( $F_{Ri}^{MVD}$ ) corresponding to each  $CMOD_i$  and for the LOP ( $F_L^{MVD}$ ), can be transformed to the corresponding loads of the 3PB test, just by a linear transformation. The transformation can generally be expressed by Eq. 3:

$$F_i^{3PB(MVD)} = k_i^{MVD} \cdot F_i^{MVD} \quad (3)$$

where  $F_i^{MVD}$  is the load obtained by the MVD test;  $k_i^{MVD}$  is *MVD transformation parameter*, a constant parameter for the transformation; and  $F_i^{3PB(MVD)}$  is the load which would be obtained by the 3PB test (as defined by the EN14651 standard). The previous three parameters are valid for both the limit of proportionality ( $i=L$ ) and the residual loads in each  $CMOD_i$  ( $i=1, 2, 3, 4$ ).

### 3 Experimental programme

The experimental campaign consisted of 22 mixes produced with different concrete matrices, types of fibres and fibre contents. These FRCs were tested by the 3PB test and the MVD test. Three to five specimens per sample were tested for every mix and test. A total of 64 3PB and 80 MVD tests were carried out.

Details of each series are described in Table 2, including the name of the series, fibre and matrix types, fibre contents, general behaviour of the FRC, control of the CMOD, type of specimen and set up in the MVD test. The previous items are described hereafter. The description of the series is given in the form “i-XX-Y-ZZ”, where “i” is a number given in sequential order; “XX” are two letters indicating the place where the tests were performed (BR: Sao Paulo University, Brazil; UY: University of the Republic, Uruguay; CH: Xi’an Jiaotong Liverpool University, China), and “Y-ZZ” describe the fibre reinforcement, where “Y” is the material of the fibres (S: Steel and P: Plastic); and “ZZ” is a number describing the fibre content in the mix, as the weight of fibres per cubic

metre of concrete ( $\text{kg/m}^3$ ). The content of fibre as a percentage of the volume of fibres over the total concrete volume is also included in the next column of the table.

Several types of concrete matrices were used. Each matrix is described by two-letter acronyms and a number. The acronyms indicate the type of matrix, meaning: Conventional concrete (CC); Self-compacting concrete (SC); Ultra high-performance concrete (UH); Micro-concrete (MC), characterized by a maximum aggregate size of 10 mm; and Sprayed concrete (SP), where the specimens were cut out from larger sprayed panels. The number indicates the nominal characteristic compressive strength ( $f_c$ ) of the mix, which ranged from 30 to 150 MPa. For these concrete matrixes and fibre content, both softening (“Soft.”) and hardening (“Hard.”) behaviour were observed for the FRC under the 3PB test.

CMOD control was directly measured by a transducer in the first series carried out (named “direct”). As previously shown, an excellent correlation was obtained between the CMOD and the stroke displacement (Eq. 2) [14]. This procedure was used to indirectly obtain the CMOD values by converting the stroke displacement measured during the test (“Indirect”).

Four different procedures were used to obtain the MVD test specimens. They are shown and represented in Fig. 3. “LB” (“*Lateral of Beams*”) specimens were obtained from one of the halves of a beam previously tested under the EN14651 test. These halves were prepared just by notching (“*LBa*”, Fig. 3a), thus obtaining a specimen of approximately ( $150 \times 150 \times 300 \text{ mm}^3$ ), or by trimming the ends of the beams to obtain a cubic specimen (150 mm wide) and then notching it (“*LBb*”, Fig. 3b). Obtaining the specimen from the beam tested under the 3PB has the advantage of testing the same material with both tests. However, it presents two disadvantages. First, the test is usually performed with some days of delay to have time to prepare the specimens. Secondly, the fibre orientation may be different, because the procedure indicated in the EN14651 standard to fill the mould aims to obtain the least altered specimen in the centre of the beam, and the mixture of different increments during filling may occur towards the side of the beam.

“CM” (“*Cubic mould*”, Fig. 3c) specimens were obtained by a direct cast of a cubic specimen 150



**Table 2** Summary of the experimental programme

Series	FRC details			MVD setup		
	Fibre content (%)	Concrete matrix	FRC behaviour	CMOD measure	Type of specimen	Wedge rotation
1-Br-S-10	0.13 <sup>a</sup>	CC-55	Soft	DIRECT	LBb	FIXED
2-Br-S-20	0.25 <sup>a</sup>	CC-55	Soft	DIRECT	LBb	FIXED
3-Br-S-30	0.38 <sup>a</sup>	CC-55	Soft	DIRECT	LBb	FIXED
4-Br-S-10	0.13 <sup>b</sup>	CC-55	Soft	DIRECT	LBb	FIXED
5-Br-S-20	0.25 <sup>b</sup>	CC-55	Soft	DIRECT	LBb	FIXED
6-Br-S-30	0.38 <sup>b</sup>	CC-55	Soft	DIRECT	LBb	FIXED
7-Ch-S-80	1.00	UH-150	Hard	INDIRECT	LBa	FIXED
8-Ch-S-160	2.00	UH-150	Hard	INDIRECT	LBa	FIXED
9-Ch-S-200	2.50	UH-150	Hard	INDIRECT	LBa	FIXED
10-Uy-S-90	1.15	SC-60	Hard	INDIRECT	PM	FIXED
11-Uy-S-35	0.44	SP-40	Soft	INDIRECT	LBa	HINGED
12-Uy-S-56	0.71	SP-40	Hard	INDIRECT	LBa	HINGED
13-Uy-S-35	0.44	MC-40	Soft	INDIRECT	CM	HINGED
14-Uy-S-35 <sup>e</sup>	0.44	MC-40	Soft	INDIRECT	LBa	HINGED
15-Uy-P-6	0.53	CC-45	Soft	INDIRECT	LBa	HINGED
16-Uy-P-12	1.26	CC-45	Soft	INDIRECT	LBa	HINGED
17-Uy-P-5	0.56	CC-30	Soft	INDIRECT	CM	FIXED
18-Uy-P-5 <sup>d</sup>	0.56	CC-30	Soft	INDIRECT	LBa	FIXED
19-Uy-P-5 <sup>d,f</sup>	0.56	CC-30	Soft	INDIRECT	LBa	FIXED
20-Uy-P-3	0.33	CC-30	Soft	INDIRECT	CM	FIXED
21-Uy-P-3 <sup>e</sup>	0.33	CC-30	Soft	INDIRECT	LBa	FIXED
22-Uy-P-3 <sup>e,f</sup>	0.33	CC-30	Soft	INDIRECT	LBa	FIXED

<sup>a</sup>Low carbon fibres

<sup>b</sup>Medium carbon fibres

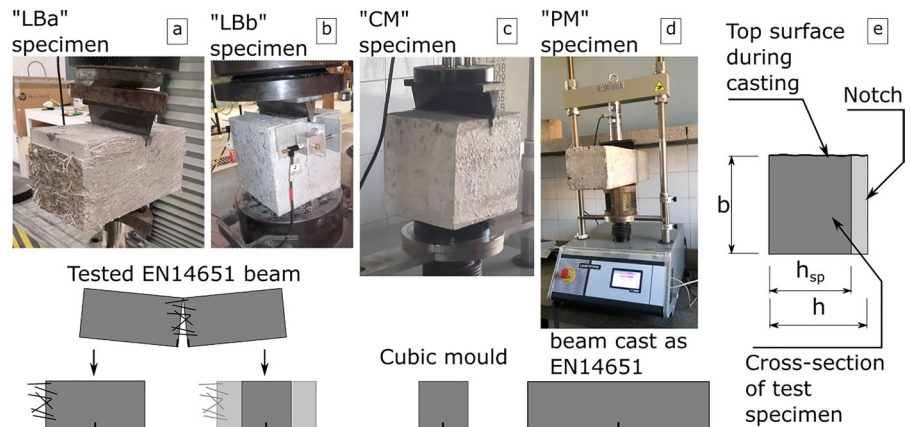
<sup>c</sup>Same set of 3PB sample than 13-Uy-S-35 series, compared with a different set of MVD sample (LBa)

<sup>d</sup>Same set of 3PB sample than 17-Uy-P-5 series, compared with a different set of MVD sample (LBa)

<sup>e</sup>Same set of 3PB sample than 20-Uy-P-3 series, compared with a different set of MVD sample (LBa)

<sup>f</sup>MVD tests were carried out using a different speed: 2 mm/min (i.e. 4 times faster than the usual speed)

**Fig. 3** Procedures to obtain MVD specimens: **a** half of the beam; **b** trimmed half of the beam; **c** cast cubic specimen; **d** cast beam specimen; **e** position of notch relative to cast



mm wide. Two advantages of this method can be mentioned. Firstly, it is a practical method as it uses small specimens. Secondly, there is less variability in how the specimens may be filled and, therefore, a similar to the 3PB fibre orientation may be expected. However, a drawback was observed in a preliminary test: cubic specimens may show odd results testing FRC with hardening behaviour, with a crack forming outside of the vertical plane. Finally, casting different specimens for the beam and the MVD tests enables performing both tests at the same age.

“PM” (“Prismatic mould”, Fig. 3d) specimens were obtained by casting a beam as indicated in EN14651. Despite being an inefficient choice for regular quality control (as it has all the drawbacks associated with the use of large specimens), it was used following the research objective of correlating both tests, as the same conditions apply for the specimens used in both tests (e.g. same material, fibre distribution and orientation). It also allows performing both tests at the same age.

In the *LB* and *PM* procedures, the specimens were obtained from, or they directly were, beams cast following EN14651. In the “CM” procedure, the cube also has the same cross-section. Specimens were rotated over 90° around their longitudinal axis or any of the two horizontal axis in the CM procedure and then sawn through the width of the specimen at mid-span (Fig. 3e). Furthermore, in all types of tests, the notch dimension results in a distance between the tip of the notch and the top of the specimen ( $h_{sp}$ ) of  $125 \pm 1$  mm. Therefore, in the four procedures, the cross-section of the MVD test is the same as the EN14651 test.

The two options of the MVD test set-ups previously described, regarding the wedge movement, were used in the different series; “hinged” when the edge was connected to the plate of the test machine through a hinge (as shown in Fig. 3a), or “fixed” where the edge was in full contact with the fixed plate of the test machine (as shown in Fig. 3b and c).

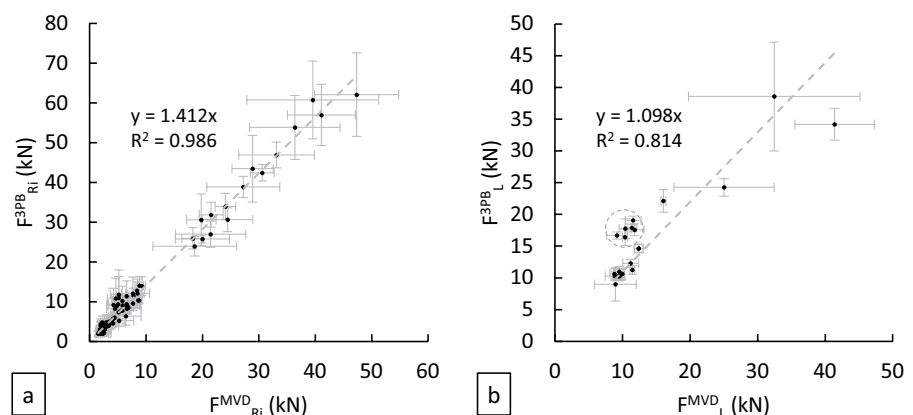
## 4 Results

### 4.1 General correlation

Figure 4a shows the residual loads obtained by the 3PB test ( $F_i^{3PB}$ ) plotted against the residual load obtained by the MVD test ( $F_i^{MVD}$ ), for each  $i=1, 2, 3$  and 4. 3PB test residual loads ( $F_i^{3PB}$ ) are as defined by EN14651. The spreadsheet containing the complete results is included as Electronic Supplementary Material (ESM) in the electronic version of the paper. In this paper, the superscript “3PB” is added to the notation given in the standard (“ $F_i$ ”) to explicitly differentiate it from the results from the MVD test. MVD test residual loads were defined in Sect. 2.3.

Each point represents the average result of the specimens tested for each series. At each point, error bars are shown, representing the standard deviation of the value for each test. As very different FRC mixes were used, the range of residual loads of the 3PB test obtained for the different series is large, ranging from around 2 to 80 kN. Correspondingly, the residual loads of the MVD ranged from around 2 to 50 kN. The best fitting line going through the origin is included in Fig. 4a. As observed, there is an excellent fit ( $R^2=0.986$ ) for the linear correlation between the

**Fig. 4** Correlation of average load from 3PB and MVD tests: **a** residual loads ( $F_{Ri}$ ); **b** limit of proportionality (LOP) loads





results of both tests. This indicates that despite very different types of FRC being involved in the analysis, a strong linear correlation was obtained between the residual loads of both tests. The excellent correlation between tests shows the robustness of the MVD test to predict 3PB results for any FRC used.

Figure 4b shows the load corresponding to the Limit of Proportionality (LOP) obtained by the 3PB test ( $F_L^{3PB}$ ) plotted against the LOP obtained by the MVD test ( $F_L^{MVD}$ ). As happened for the residual loads, each point represents the average of the specimens tested in the series. Standard deviation and the best fitting line are also included. Although a good correlation still exists between the results, the correlation coefficient was lower ( $R^2=0.814$ ) than for the residual loads. This could be associated with the lower number of average results as we have just one LOP value achieved in each test against four residual strength values. Also, there is a cluster of values (highlighted with a dotted circle) corresponding to series 1–6 (Brazilian Experimental program) which fall outside the general trend. This could be caused by the specificity of the test machine support apparatus. Despite the lower correlation, this is still an advance, as no correlation was found for the LOP in previous studies analysed.

The experimental value of  $k_i^{MVD}$  can be obtained from the slope of each of the plots in Fig. 4:  $k_L^{MVD}=1.098$ , and  $k_{Ri}^{MVD}=k_{R1}^{MVD}=k_{R2}^{MVD}=k_{R3}^{MVD}=k_{R4}^{MVD}=1.412$ . Based on the results, and introducing a negligible error ( $<1\%$ ) for the sake of simplicity, the following *MVD transformation parameters* are proposed to be used in practice:  $k_L^{MVD}=1.1$  for the LOP and  $k_{Ri}^{MVD}=1.4$  for all the  $CMOD_i$  of the residual loads used in practice ( $i=1, 2, 3, 4$ ). Considering these factors, Eq. 3 yields the following correlation equations (Eqs. 4 and 5), which can be used in practice:

$$F_{Ri}^{3PB(MVD)} = 1.4 \cdot F_{Ri}^{MVD} \quad (4)$$

$$F_L^{3PB(MVD)} = 1.1 \cdot F_L^{MVD} \quad (5)$$

The change in the *MVD transformation parameter* from the LOP to the residual loads is coherent with the change in behaviour of the specimen, after the concrete matrix cracks.

#### 4.2 Analysis of correlation factor by parameters

The analysis of the correlation made in general to all the series in Sect. 4.1 was repeated for the residual loads ( $F_i^{3PB}$  and  $F_i^{MVD}$ ) of each of the  $CMOD_i$

**Table 3** *MVD transformation parameter for different test parameters*

Parameter	Value	n	$k^{MVD}$	$\Delta k^{MVD}(\%)$	$R^2$
General	All values	88	1.412	0.0	0.986
CMOD <sub>i</sub>	i = 1 (0,5 mm)	22	1.413	0.1	0.990
	i = 2 (1,5 mm)	22	1.404	-0.6	0.989
	i = 3 (2,5 mm)	22	1.430	1.3	0.983
	i = 4 (3,5 mm)	22	1.401	-0.7	0.972
Country	Brazil	24	1.463	3.6	0.665
	Uruguay	52	1.366	-3.3	0.975
	China	12	1.420	0.5	0.980
Behaviour	Hardening	20	1.408	-0.2	0.981
	Softening	68	1.448	2.6	0.765
Wedge rotation	Hinged	24	1.476	4.5	0.921
	Fixed	64	1.408	-0.2	0.987
Type of MVD specimen	CM	12	1.364	-3.4	0.944
	PM	4	1.318	-6.7	0.975
	LBa	48	1.424	0.8	0.993
	LBb	24	1.463	3.6	0.665
Type of fibre	Steel	56	1.413	0.0	0.984
	Plastic	32	1.375	-2.6	0.797



( $i=1, 2, 3, 4$ ) and for groups of results the same value of a certain property of the test (e.g. Country, Behaviour, etc.). The results are summarized in Table 3. The table shows the number of points ( $n$ ) that form each group, the *MVD transformation parameter* ( $k^{MVD}$ ) obtained for that group, and the difference in percentage in the *MVD transformation parameter* obtained for that group ( $\Delta k^{MVD}$ ), compared to the general *MVD transformation parameter* ( $k_i^{MVD}=1.412$ ) obtained in Sect. 4.1, and the strength of the correlation (given by Pearson correlation coefficient:  $R^2$ ).

Very similar *MVD transformation parameters* were obtained for all the series, although this comparison is not based on rigorous analysis, as series with a different number of points and ranges are compared. The largest differences were 3.6% above or 6.7% below the general *MVD transformation parameter*. If the results are grouped for different CMODs, the relative difference, in percentage, of the *MVD transformation parameter* with the general *MVD transformation parameter*, is smaller than 2%. This means it is valid to use the same *MVD transformation parameter* for all the residual strengths corresponding to different  $CMOD_i$  usually used ( $i=1, 2, 3, 4$ ).

Similar results are obtained analysing the other parameters, such as country of testing ( $\Delta k^{MVD} < 3.6\%$ ), the behaviour of the FRC ( $< 2.6\%$ ), the wedge rotation ( $< 4.5\%$ ), the type of specimen ( $< 6.7\%$ ), and the type of fibre ( $< 2.6\%$ ). Obtaining a similar *MVD transformation parameter* ( $k^{MVD}=1.4$ ) despite the very different test set up were used, and performing the test in three different countries, demonstrates the robustness of the MVD test. This is a major advantage of the test compared with other tests,

which need a tailored correlation for each mix and CMOD, or an even less accurate general correlation [17, 21, 23].

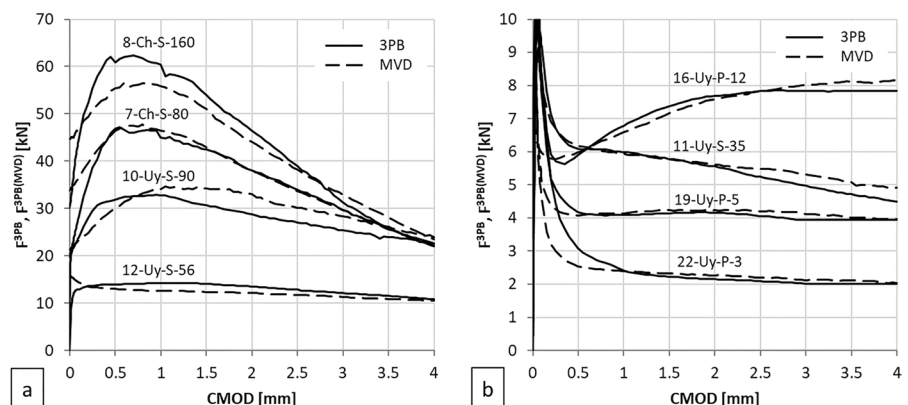
All the series showed a good to excellent correlation, most of them with  $R^2$  above 0.90. The worst correlation ( $R^2=0.665$ ) was obtained in the tests carried out in Brazil, coinciding with the only campaign made with the “LBb” type of specimens. The series with the lower correlation ( $R^2=0.665$ ) still show a similar *MVD transformation parameter* ( $\Delta k^{MVD}=3.6\%$ ).

#### 4.3 Individual series behaviour

Individual results for different series are shown in Fig. 5. The figure simultaneously shows the average load vs CMOD plot obtained by the 3PB tests (continuous lines) and by the MVD test (dashed lines); the latter corrected by the *MVD transformation parameter* for residual loads (Eq. 4). Four series with hardening behaviour (Fig. 5a) and four with softening behaviour (Fig. 5b) were chosen to represent all the range of strengths tested, including mixes with both plastic (P) and steel (S) fibres. Note the scales of the plots, which include results with residual loads ranging from 10 to 70 kN for the results with hardening, and from 2 to 9 kN for the results with softening.

Besides the excellent quantitative correspondence shown in the previous section, it can now be visually observed that the corrected MVD test results also show a qualitative correspondence with the 3PB test, capturing the different increments and reductions of the residual loads for the wide range of FRC mixes tested. The correspondence seems more precise for the results with softening behaviour (Fig. 5b).

**Fig. 5** Comparison of Individual behaviour of 3PB and corrected MVD test: **a** hardening FRC, **b** softening FRC



As depicted by the *fib* Model Code [8] and previous research [33], the same mix of FRC can show a different response depending on the testing method. For example, a FRC mix can present softening if it is tested under uni-axial tensile tests or hardening if it is tested under a bending test. The MVD test works as a combined mode between flexion and tension and, therefore, a FRC mix may also show a change in response if tested with an MVD or 3PB test, as previously described.

It is thus also worth mentioning the case of series 12-Uy-S-56, which reflects the nature of the MVD test. In this series, the result from the 3PB test showed a barely hardening behaviour, with a  $F_{R1}$  value (13.97 kN) just above the  $F_{LOP}$  value (12.30 kN). In turn, the results of the MVD test show a value of  $F_{R1}^{MVD}$  (9.27 kN) below the  $F_L^{MVD}$  value (11.20 kN), which would correspond to a softening behaviour. However, if the MVD test results are corrected by the correction factors (Eqs. 4 and 5), it shows a value of  $F_{R1}^{3PB(MVD)}$  (13.09 kN) and  $F_L^{3PB(MVD)}$  (12.30 kN) corresponding to a hardening behaviour of the 3PB test. Therefore, also regarding the hardening and softening behaviour, the MVD test can predict the correct behaviour of the 3PB test.

Figure 6 shows two specimens at the end of the 3PB test and two after the MVD test (inverted). Similar cracking patterns are obtained with both tests. In the MVD test, the cracks started at the notch tip and subsequently propagated smoothly towards the base of the specimen. A progressive and stable formation of cracks was observed during the tests, even for low fibre contents, whereby the 3PB test is more susceptible to cracking instabilities. The MVD test can also register the different types of cracks which are usually registered by the 3PB test. From the more straight, single-branched crack associated with FRC with

lower fibre contents, to cracks with several branches and increased tortuosity, associated with FRC with higher fibre contents.

#### 4.4 Scatter of results

The Coefficient of Variation (CV), in percentage, of the 3PB against the CV of the MVD tests is plotted in Fig. 7. Each point represents the average CV ( $CV_{ave}$ ) of a group of results, which are defined by the value of the residual load corresponding to the 3PB test. The range of values of each group is included in a label next to each point. The number of values of each group (n) is also shown. Two points representing the CV of the LOP are also included.

In general, the range of the CV for the residual loads is between 10 and 30%, which is the usual range for FRC [23, 34]. For large residual loads (usually associated with more fibre content), results show less scatter

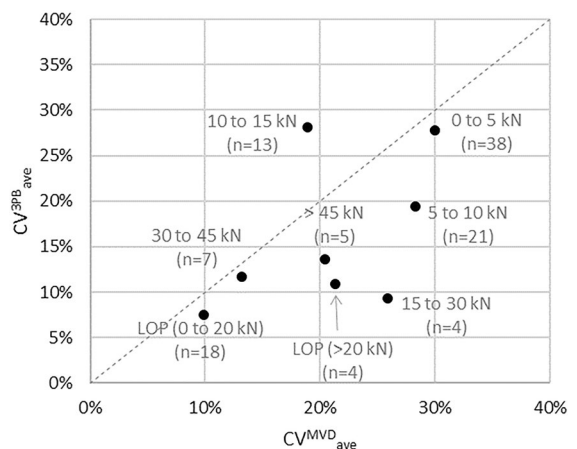


**Fig. 7** Correlation of average coefficients of variation (CV) obtained for the results with each test

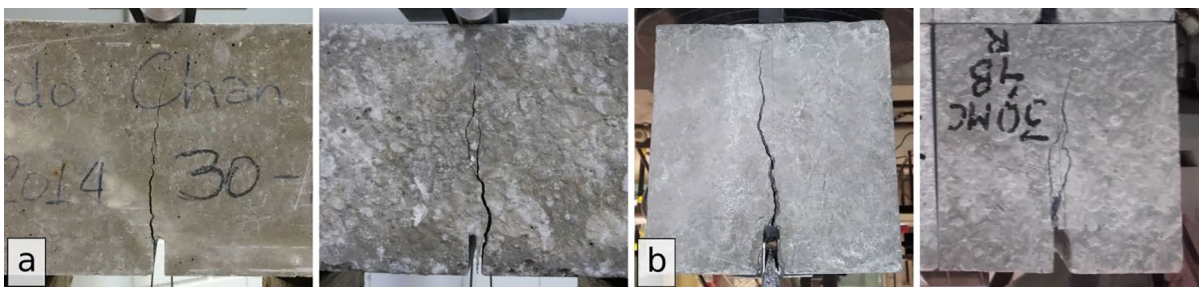


**Fig. 6** Cracking patterns: **a** 3PB tests; **b** MVD tests (inverted)

than for low fibre content. The LOP is mainly governed by the tensile strength of the concrete matrix, which usually has a smaller scatter than the residual loads in FRC. This was observed for the series with LOP smaller than 20 kN, which had a CV smaller than 10%, whereas the series with larger LOP showed a larger standard deviation. Also, for large LOP values, the scatter is particularly large in the results from the MVD test (above 20%), probably due to the aforementioned difficulties to accurately evaluate the cracking point.

Comparing both tests, it can be seen that for the LOP series and all the series of residual strength but one (10–15 kN), the MVD test shows a larger average CV (more points below the identity line). Considering all data, the average CV in the MVD test is 3.9% larger in LOP, and 3.0% larger in residual loads, than in the 3PB test.

With the results from this paper, it seems that the average value for the LOP and residual loads of any FRC mix can be appropriately determined using the MVD test, with an error similar to the one obtained by the 3PB test. Thus, for the design of elements based on the average results (such as industrial pavements designed by the TR34), the MVD test may be used in the current state. In turn, although the estimation of the characteristic values of the FRC mix is still possible by the MVD test, it would give conservative values as the MVD test shows a slightly higher dispersion than that obtained by the 3PB test. More research should be done into this aspect to correctly correlate the dispersion obtained by both tests, allowing predicting the characteristic values more precisely.

## 5 Design and control of FRC based on MVD test

The limit of proportionality (LOP) and residual flexural tensile strengths ( $f_{R,i}$ ), according to the 3PB test given by EN14651, can be obtained by the MVD test using the equations given in the standard and the correlation equations described in this paper, as follows.

The limit of proportionality (LOP),  $f_{ct,L}^f$ , in Newton per square millimetre, is given by the expression:

$$f_{ct,L}^f = \frac{3F_L l}{2bh_{sp}^2} = 1.65 \frac{F_L^{MVD} l}{bh_{sp}^2} \quad (6)$$

where  $F_L$  is the load corresponding to the LOP, in Newton, which can be obtained by the MVD test

through Eq. 5 ( $F_L = F_L^{3PB(MVD)} = 1.1 \cdot F_L^{MVD}$ );  $l$  is the nominal span length of the EN14651 test, in millimetres ( $l = 500\text{mm}$ );  $b$  is the width of the specimen, in millimetres; and  $h_{sp}$  is the distance between the tip of the notch and the top of the specimen, in millimetres.

Accordingly, the residual flexural tensile strengths  $f_{R,i}$  are given by the expression:

$$f_{R,j} = \frac{3F_i l}{2bh_{sp}^2} = 2.1 \frac{F_{Ri}^{MVD} l}{bh_{sp}^2} \quad (7)$$

where  $F_i$  is the load corresponding to  $CMOD = CMOD_i$  ( $i = 1, 2, 3, 4$ ), in Newton, which can be obtained by the MVD test through Eq. 4 ( $F_i = F_{Ri}^{3PB(MVD)} = 1.4 \cdot F_{Ri}^{MVD}$ );  $l$  is the nominal span length of the EN14651 test, in millimetres ( $l = 500\text{mm}$ );  $b$  is the width of the specimen, in millimetres; and  $h_{sp}$  is the distance between the tip of the notch and the top of the specimen, in millimetres.

Figure 8 shows the strengths ( $f_i^{3PB}$ ) calculated according to EN14651 standard, using the 3PB test, plotted against the strengths ( $f_i^{MVD}$ ) calculated by Eqs. 6 and 7 using the results of the MVD test. Nominal values were employed in the calculations ( $L=500$  mm;  $h_{sp}=125$  mm and  $b=150$  mm) since the errors in the dimensions of the samples were, in most cases,  $<2\%$ . Each point represents the average result of the specimens tested for each series, both for the residual strengths ( $f_{R,j}$ , shown in Fig. 8a) and for the LOP ( $f_{ct,L}$ , shown in Fig. 8b). The best fitting line passing through the origin is included in Fig. 8.

In both cases, the best-fitting line closely aligns with the identity line ( $y=x$ ), indicating that, for a specific FRC, similar strengths can be achieved using both the 3PB test and the MVD test. Furthermore, there is an excellent ( $R^2=0.986$ ) and a good ( $R^2=0.814$ ) linear correlation between the results of both tests for the residual strengths and LOP, respectively.

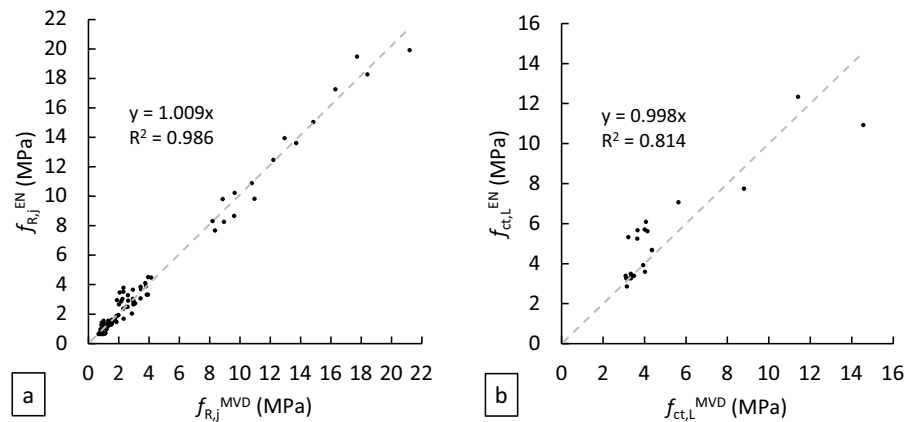
Hence, the MVD test can be directly used for the design or quality control of FRC elements, following the codes or recommendations that use the EN14651 standard (e.g. Model Code 2010, TR34, EHE-08, ABNT NBR 16935).

## 6 Conclusions

A new configuration of the wedge splitting test, the so-called Montevideo (MVD) test, to evaluate the



**Fig. 8** Correlation of average strength, calculated from 3PB and MVD tests: **a** Residual flexural tensile strengths ( $f_{R,i}$ ); **b** Limit of Proportionality (LOP) strengths



tensile properties of FRC is analysed. This paper presents the results from several experimental campaigns carried out in three different countries to obtain the qualitative and quantitative equivalence between the MVD test and the 3PB test. The following conclusions can be drawn:

A single set of correlation equations was obtained between the MVD test and 3PB test, based on a linear transformation of the MVD test displacements into the CMOD (Eq. 2), and a linear transformation for both the proportional load (Eq. 5) and the residual loads (Eq. 4), which is valid for all the  $CMOD_i$  ( $i = 1, 2, 3, 4$ ) evaluated in the EN14651 standard.

The same set of correlation equations was shown to be valid for all the different types of concretes (which included conventional, Self-Compacting, Ultra High-Performance, Micro and Sprayed concrete, with nominal characteristic compressive strengths ranging from 30 to 150 MPa), blended with different fibre types and contents (from 2 kg/m<sup>3</sup> of plastic fibres to 200 kg/m<sup>3</sup> of steel fibres), resulting in both softening and hardening behaviour, with tests carried out in three countries, using different equipment, test set-up and types of testing specimens.

The corrected MVD test results show an excellent quantitative correspondence with the 3PB test, showing a very similar *MVD transformation parameter* for all the series studied. Also, it showed a qualitative correspondence, capturing the different increments and reductions of the residual loads for the wide range of FRC mixes tested. Furthermore, similar cracking patterns are obtained in the specimens with both tests.

Therefore, it seems that, in contrast with other simplified tests, a general set of correlation equations (for any FRC used) was obtained to convert the results from the MVD test to the 3PB test. This correlation equations covers all the parameters used to obtain constitutive equations, which emphasizes the ability of the MVD test to be used as an instrument for FRC quality control for structural purposes. The correlation can be used to obtain, in a simplified way with the MVD test, the Limit of Proportionality (Eq. 6) and the residual tensile strengths (Eq. 7) of FRC as obtained by the EN14651 standard. It allows the design, characterization, and control of FRC mixes based on new recommendations, such as *fib* Model Code, TR34, EHE-08, SS 674, or ABNT NBR 16935.

**Acknowledgements** The authors thankfully acknowledge the financial support of São Paulo Research Foundation (*Fundação de Amparo à Pesquisa do Estado de São Paulo*, FAPESP. *Processo: 2016/05255-5*) for funding this research. L.S.-C. thanks Ame and Seba for the contribution to the statistical analysis. R. M. would like to acknowledge the financial support of the National Council for Scientific and Technological Development—CNPq (Proc. N°: 437143/2018-0). A. F. gratefully acknowledges the CNPq for the support (Proc. N°: 305055/2019-4).

**Author contributions** LSC: conceptualization; data curation; formal analysis; methodology; experimental tests; original draft. RM and IG: experimental tests. AF: supervision. All authors: writing—review and editing.

**Data availability** The raw data required to reproduce these findings is available online in the electronic version of the paper as Electronic Supplementary Material (ESM) and can also be accessed in the Udelar repository at: <https://www.colibri.udelar.edu.uy/jspui/handle/20.500.12008/43189>



## Declarations

**Conflict of interest** The authors declare that they have no known competing financial interests or personal relationships that could have appeared to influence the work reported in this paper.

## References

- Trindade YT, Bitencourt LAG, Manzoli OL (2020) Design of SFRC members aided by a multiscale model: part II—predicting the behavior of RC-SFRC beams. *Compos Struct* 241:112079. <https://doi.org/10.1016/j.compstruct.2020.112079>
- de Figueiredo AD, Ceccato MR (2015) Workability analysis of steel fiber reinforced concrete using slump and Ve-Be test. *Mater Res* 18:1284–1290. <https://doi.org/10.1590/1516-1439.022915>
- Blanco A, Pujadas P, de la Fuente A, Cavalaro S, Aguado A (2013) Application of constitutive models in European codes to RC-FRC. *Constr Build Mater* 40:246–259. <https://doi.org/10.1016/j.conbuildmat.2012.09.096>
- 544.1R-96 (2009) Report on fiber reinforced concrete (reapproved 2009), American Concrete Institute
- ABNT, ABNT NBR 16935 (2021) Projeto de estruturas de concreto reforçado com fibras—Procedimento
- Standards Australia (2018) AS 3600:2018—Concrete structures
- SS 674 (2021) Fibre concrete—design of fibre concrete structures. Singapore Standard, Singapore Standards Council. [www.sis.se](http://www.sis.se)
- FIB, fib Model Code for Concrete Structures 2010 (2013) Fédération Internationale du Béton, Lausanne
- di Prisco M, Plizzari G, Vandewalle L (2009) Fibre reinforced concrete: new design perspectives. *Mater Struct* 42:1261–1281. <https://doi.org/10.1617/s11527-009-9529-4>
- Louch K (1995) Technical report 34 concrete industrial ground floors: a guide to design and construction. The Concrete Society, London
- CPH, EHE-08: Instrucción del Hormigón Estructural (in Spanish), 2008.
- Aldrian W, Thomas A, Chittenden N, Holter KG (2020) ITA REPORT N°24. Permanent sprayed concrete linings (ITA.WG.12 & ITAtech), ITA-AITES
- EN 14651:2007+A1:2008 (2008) Test method for metallic fibre concrete—Measuring the flexural tensile strength (limit of proportionality (LOP), residual)
- Segura-Castillo L, Monte R, De Figueiredo AD (2018) Characterisation of the tensile constitutive behaviour of fibre-reinforced concrete: a new configuration for the Wedge Splitting Test. *Constr Build Mater* 192:731–741. <https://doi.org/10.1016/j.conbuildmat.2018.10.101>
- Molins C, Aguado A, Saludes S (2009) Double Punch Test to control the energy dissipation in tension of FRC (Barcelona test). *Mater Struct* 42:415–425. <https://doi.org/10.1617/s11527-008-9391-9>
- di Prisco M, Ferrara L, Lamperti MGL (2013) Double edge wedge splitting (DEWS ): an indirect tension test to identify post-cracking behaviour of fibre reinforced cementitious composites. *Mater Struct* 46:1893–1918. <https://doi.org/10.1617/s11527-013-0028-2>
- Galeote E, Blanco A, Cavalaro SHP, de la Fuente A (2017) Correlation between the Barcelona test and the bending test in fibre reinforced concrete. *Constr Build Mater* 152:529–538. <https://doi.org/10.1016/j.conbuildmat.2017.07.028>
- Martinelli P, Colombo M, de la Fuente A, Cavalaro S, Pujadas P, di Prisco M (2021) Characterization tests for predicting the mechanical performance of SFRC floors: design considerations. *Mater Struct Constr* 54:1–16. <https://doi.org/10.1617/s11527-020-01598-2>
- Simão LDCR, Nogueira AB, Monte R, Salvador RP, de Figueiredo AD (2019) Influence of the instability of the double punch test on the post-crack response of fiber-reinforced concrete. *Constr Build Mater* 217:185–192. <https://doi.org/10.1016/j.conbuildmat.2019.05.062>
- Borges LAC, Monte R, Rambo DAS, de Figueiredo AD (2019) Evaluation of post-cracking behavior of fiber reinforced concrete using indirect tension test. *Constr Build Mater* 204:510–519. <https://doi.org/10.1016/j.conbuildmat.2019.01.158>
- Estrada Cáceres AR, Cavalaro SHP, Monte R, de Figueiredo AD (2021) Alternative small-scale tests to characterize the structural behaviour of steel fibre-reinforced sprayed concrete. *Constr Build Mater* 296:123168. <https://doi.org/10.1016/j.conbuildmat.2021.123168>
- Galobardes I, Silva CL, Figueiredo A, Cavalaro SHP, Goodier CI (2019) Alternative quality control of steel fibre reinforced sprayed concrete (SFRSC). *Constr Build Mater* 223:1008–1015. <https://doi.org/10.1016/j.conbuildmat.2019.08.003>
- Conforti A, Minelli F, Plizzari GA, Tiberti G (2018) Comparing test methods for the mechanical characterization of fiber reinforced concrete. *Struct Concr* 19:656–669. <https://doi.org/10.1002/suco.201700057>
- Bernard ES (2002) Correlations in the behaviour of fibre reinforced shotcrete beam and panel specimens. *Mater Struct* 35:156–164. <https://doi.org/10.1007/BF02533584>
- Estrada Cáceres AR, Pialarissi Cavalaro SH, Domingues de Figueiredo A (2021) Evaluation of steel fiber-reinforced sprayed concrete by energy absorption tests. *J Mater Civ Eng* 33:1–11. [https://doi.org/10.1061/\(asce\)jmt.1943-5533.0003865](https://doi.org/10.1061/(asce)jmt.1943-5533.0003865)
- Tschegg EK (1986) Equipment and appropriate specimen shape for tests to measure fracture values. Patent AT-390328
- Gopalaratnam VS, Gettu R (1995) On the characterization of flexural toughness in fiber reinforced concretes. *Cem Concr Compos* 17:239–254
- Banthia N, Islam ST (2013) Loading rate concerns in ASTM C1609. *J Test Eval* 41:20120192. <https://doi.org/10.1520/JTE20120192>
- Molins C, Aguado A, Saludes S (2008) Double punch test to control the energy dissipation in tension of FRC (Barcelona test). *Mater Struct* 42:415–425. <https://doi.org/10.1617/s11527-008-9391-9>
- Pujadas P, Blanco A, Cavalaro S, de la Fuente A, Aguado A (2013) New analytical model to generalize the barcelona test using axial displacement. *J Civ Eng Manag*



- 19:259–271. <https://doi.org/10.3846/13923730.2012.756425>
31. Segura-Castillo L, García N, Figueredo D, Clavijo A, González E, Muniz B, Rodríguez I, Rodríguez G (2022) Recent FRC developments in Uruguay: quality control, durability and three structural applications. In: PS et al (ed) BEFIB2021—RILEM Bookseries 36. Springer International Publishing, Valencia, pp 739–748. [https://doi.org/10.1007/978-3-030-83719-8\\_63](https://doi.org/10.1007/978-3-030-83719-8_63)
32. Rossi P, Brühwiler E, Chhuy S, Jenq YS, Shah SP (1991) Fracture properties of concrete as determined by means of wedge splitting tests and tapered double cantilever beam tests. In: Surendra Shah AC (ed) Fracture mechanics test methods for concrete. Taylor & Francis Group, London, pp 87–128
33. Cominoli L, Meda A, Plizzari GA (2007) Fracture properties of high-strength hybrid fiber-reinforced concrete. In: Grosse CU (ed) Advances in construction materials. Springer, Berlin, pp 139–146
34. Cavalaro SHP, Aguado A (2014) Intrinsic scatter of FRC: an alternative philosophy to estimate characteristic values. Mater Struct 48:3537–3555. <https://doi.org/10.1617/s11527-014-0420-6>

**Publisher's Note** Springer Nature remains neutral with regard to jurisdictional claims in published maps and institutional affiliations.

Springer Nature or its licensor (e.g. a society or other partner) holds exclusive rights to this article under a publishing agreement with the author(s) or other rightsholder(s); author self-archiving of the accepted manuscript version of this article is solely governed by the terms of such publishing agreement and applicable law.